International Journal of Engineering & Technology, 7 (3.17) (2018) 186-190

International Journal of Engineering & Technology

Website: www.sciencepubco.com/index.php/IJET

Research paper

Microstructure, Mechanical Properties and Fatigue Behavior of AlSi10Mg: an Additive Manufacturing Material

Muhamad Aqil Azri[1]*, Mohd Shamil Shaari [1,2], Ahmad Kamal Ariffin[1*] Shahrum Abdullah[1]

[1]Centre for Integrated Design for Advanced Mechanical System (PRISMA), Faculty of Engineering and Built Environment, Universiti Kebangsaan Malaysia,43600 Bangi, Selangor, Malaysia
[2]Faculty of Engineering Technology, Universiti Malaysia Pahang, Lebuhraya Tun Razak, 26600 Gambang, Pahang, Malaysia.
**Corresponding author E-mail: kamal3@ukm.edu.my*

Abstract

The additive manufacturing using direct metal laser sintering (DMLS) is currently gaining interest among researchers. This is due to its potential to improve the manufacturing process in the aerospace and automotive industries. This paper aims to analyse the mechanical properties, microstructure and fatigue behaviour for both conditions, as-built and heat-treated (T6). The microstructure of the as-built specimen shows ultra-fine grain boundaries whereas the heat-treated specimen showing homogenous and coarsened microstructure. The ultimate tensile strength for the as-built specimen is 392 MPa whilst the heat-treated (T6) specimen is recorded at 287 MPa. The heat-treated specimen exhibiting a significant improvement in fatigue life in all range of stresses compared to as-built during fatigue testing. Hence, the heat-treatment does improve the material characteristics as well as the fatigue behaviour. Nonetheless, more researches are needed to enhance the integrity of the AlSi10Mg produced by additive manufacturing.

Keywords: *Additive Manufacturing; Fatigue Behavior; Metal Laser Sintering; Mechanical Properties; Microstructure Properties.*

1. Introduction

Various manufacturing industries are now benefiting from the additive manufacturing (AM) technology due to complex structural designs are able to be manufactured using metal materials. This is because of the advantages of AM technology for being able to build components with complex geometry by adding the materials instead of subtracting the materials like conventional methods such as computer numerical control (CNC). The AM technology is known for product development, thus the other name for AM is rapid prototyping. Today, the AM is not only used to manufacture prototypes but it is used to manufacture end-products (final parts). This is because the metal materials are now can be used by AM technology in product manufacturing and development.
Therefore, the AM technology is rapidly generating popularity not only in manufacturing industries but also to researchers. Teaming up with several universities around the world, the large manufacturing companies such as Boeing, GE, Airbus and many other automotive companies are starting to established and manufacturing numerous end-products [1-3]. The AM technology fulfils the manufacturing goals by shortening the processes thus shortening the supply chains that lead to lower total manufacturing time while increasing the production rates proportionally. Several studies have been produced by other researchers in particular to AM materials such as for TiAl6V4 material [4, 5], SS316L material [6] and AlSi10Mg material [7-10].
However, the lack of integrity analysis of the AM material and the components produced by AM technology is the main concern. This is due to the facts that it is related closely to the human safety especially when the components are used in automotive or public transports. Hence, the structural integrity analysis is used to study the components produced by AM technology. For many decades, the structural integrity analysis has become a challenge for engineers to overcome. This is due to the existence of crack due to fatigue phenomenon arises from the cyclic stresses [11, 12]. Although after than four decades, the fatigue and fracture behaviour is still considered as a critical area for researchers since it is related closely to human safety.
Based on the literature, the number of researches in investigating the structural integrity of the AM material is still considered below par compared to the rapid growth in the AM applications in the industries. Furthermore, the most of the researches are using the AlSi10Mg material, but the components are produced by selective laser melting (SLM) method. Therefore, this paper aims to determine the integrity of the AM components using AlSi10Mg material produced by DMLS method. This is including the material properties and characteristics, microstructural behaviour and fatigue behaviour.

2. Experimental Procedures

Figure 1 is showing the methodology in the form of a flowchart that is used in this study. Specimens were fabricated using direct laser metal sintering (DMLS) machine. Then, heat-treatment (T6) is subjected to a batch of fabricated specimens. Microstructural characterization is conducted to observe the microstructure on the surface of the specimen. The specimen underwent various preparation procedures prior to microstructural analysis. This includes mounting, grinding, polishing and etching of materials. Microstructural analysis was carried out using two types of microscopes which are optical microscope and scanning electron microscope (SEM).

Copyright © 2018 Authors. This is an open access article distributed under the Creative Commons Attribution License, which permits unrestricted use, distribution, and reproduction in any medium, provided the original work is properly cited.

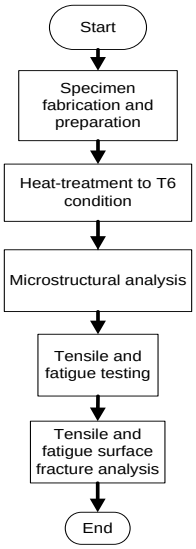


Fig 1: Methodology.

For the tensile test, universal testing machine (UTM) is used for determining the mechanical properties of the as-built material and heat-treated material. The test was conducted following the ASTM-E8 standard with strain rate and overhead speed of 1.8 mm/m and 1 x 10-3 s-1 respectively. In addition, the fatigue test was performed using an Instron testing machine. Fatigue tests were conducted in a stress-controlled testing mode following the ASTM-E466 standard. Tests were conducted in atmospheric air at room temperature. The cyclic loading followed a sine wave. The frequency used is 15 Hz and the R-value of 0.1. Finally, the fracture surface of the specimen both from tensile and fatigue tests are observed and analysed using an optical microscope respectively.

2.1. Design of fabricated specimen made for testing

There are two types of tests in this study, namely the tensile test and fatigue test. Different designs of the specimen are fabricated for both of the test based on ASTM standard mentioned previously. Figure 2 (a) represents the drawing for tensile specimens with 30 mm gauge length and 6 mm diameter. The neck is fillet with a 15 mm radius to reduce the stress concentration when it is subjected to tensile loading. Figure 2 (b) shows the drawing of fatigue specimen, build with continues radius of 15 mm and a diameter of 6 mm. The specimens were manufactured using DMLS machine by EOS M290. It is built vertically, perpendicular to the build platform and. The specimens were ground and polished as well as examining for major defects such as voids and visible cracks prior to mechanical tests.

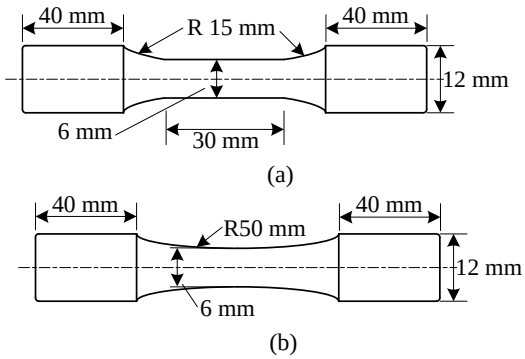


Fig 2: Schematics of fabricated specimens for (a) tensile test (b) fatigue test.

3. Results and Discussion

Experimental results obtained from the characterization of the microstructure, tensile test, fatigue tests on AlSi10Mg specimens are discussed. The microstructural analysis consists of two parts which are the observation of the fracture surface and chemical composition mapping using a scanning electron microscope (SEM). The effects of heat treatment for the T6 condition on the microstructure of the specimens are discussed. In addition, this section also discusses the mechanical properties of the alloy AlSi10Mg. The results of tensile and fatigue tests of materials (as-built and heat-treated) are presented and compared.

3.1. Microstructure of as-built AlSi10Mg

According to Thijs, et al. [13], the microstructure of AlSi10Mg manufactured using AM process can be divided into three zones: namely, the melt pool, melt pool boundary and heat affected zone. Manfredi, et al. [14] also mentioned the microstructural features that are typical of the AM material produced by AM process. Figure 3 shows the microstructure of AlSi10Mg specimen through an optical microscope. In this figure, the core of the melt pool and the melt pool boundary can be seen clearly. Ultra-fine grains can be observed in the core of the melt pool.
However, coarser grains are seen on the melt pool boundary. It also has a columnar morphology indicating cellular-dendritic growth during solidification. This is attributed to the region being in contact with readily solidified Al that has lower thermal conductivity imposing slower solidification. When the liquid metal solidifies on a flat solid surface, unidirectional solidification is adopted rather than equiaxed solidification [9]. Figure 4 shows the composition map for elements on the surface of the specimen. It can be seen that the composition of the aluminium is dominant compared to silicon. This is because the coarsening of Al at the melt pool of boundaries reduces the fraction of grain boundaries in the area. This led to a reduction of sites where the segregation of Si occurs.

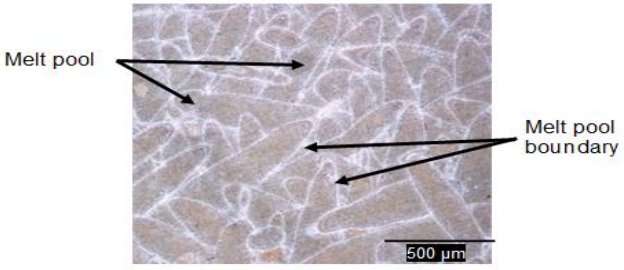


Fig 3: Microstructure of as-built AlSi10Mg.

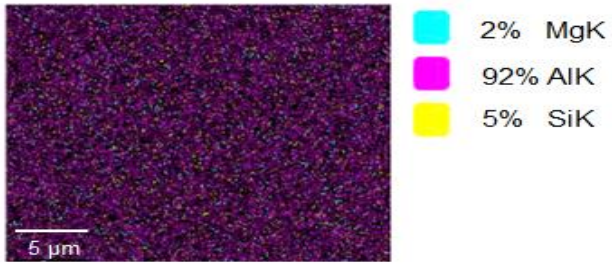


Fig 4: Chemical composition of as-built AlSi10Mg.

3.2. Microstructure of heat-treated (T6) AlSi10Mg

Figure 5 shows a homogeneous and uniform microstructure after the specimen underwent heat treatment (T6). In this study, the specimen is heat-treated based on peak hardening method. In peak hardening, solution heat treatment (SHT) involves maintaining the material at an elevated temperature (520 ºC) for a duration long enough in order to obtain a homogenous supersaturated solid solu-

tion after quenching [10]. The material then undergoes an artificial ageing process at a temperature of 165 ºC for 7 hours. After the specimen underwent SHT, the microstructure coarsened and Si started diffusing to form particles (spheroidisation). High temperature imposed during the heat treatment process provides the necessary activation energy for the diffusion of Si. Figure 6 shows the composition map for chemical elements in AlSi10Mg and confirmed that the diffusion of Si to form particles (spheroidisation).

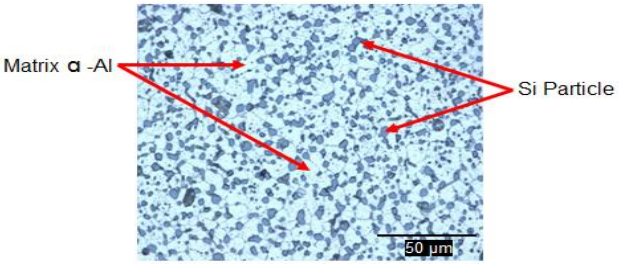


Fig 5: Microstructure of heat-treated (T6) AlSi10Mg

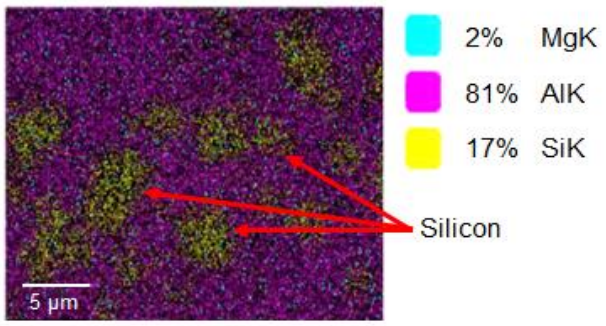


Fig 6: Chemical composition of heat-treated (T6) AlSi10Mg.

3.3. Tensile test

Table 1 is showing the overall tensile test results for both as-built and T6 specimen. It was found that there is a reduction in ultimate tensile strength (UTS), yield strength, and modulus of elasticity of the heat-treated (T6) compared to as-built specimens. Figure 7 shows the results that are obtained from a tensile test using as-built and heat-treated (T6) specimens. The specimens exhibiting brittle behaviour under quasi-static loading and the amount of strain recorded is shyly above 3%. The yield strength for the as-built specimen is showing 233.2 MPa while the ultimate tensile strength (UTS) is recorded at 391.9 MPa. For the heat-treated specimens, it shows a reduction in terms of maximum strength of the material. In contrast, the ductility of the material was found to have improved. It can be seen that the strain increases by 6.6%. The yield strength of the specimen is 226.9.0 MPa and the ultimate strength of the specimen decreased to 287.2 MPa. Overall, the UTS of heat-treated specimens is reduced by almost 30% when compared to as-built. However, the ductility of the T6 specimens is improved by a factor of 1.375. Similar behaviour between as-built and T6 specimens are also presented by [9, 15] in their study. It is because of when the specimen is undergoing SHT to T6 condition, the material is experiencing annealing hence, softening the material compared to as-built.

Table 1: Overall tensile test results

AlSi10Mg Specimens	Yield Strength, 0.2 % offset (MPa)	Modulus of Elasticity (GPa)	Ultimate Tensile Strength (MPa)	Strain (%)
As-built	233.0	62.0	392.0	4.8
Heat-treated	227.0	74.0	287.0	6.6

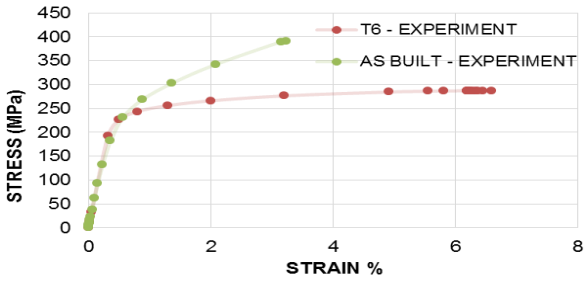


Fig 7: Tensile graph of as-built AlSi10Mg.

From the tensile testing, it is difficult to categorize these specimens as ductile or brittle materials by the observing the amount of strain only [16]. Therefore, the observations of the fracture surface of the specimen are conducted. According to [17], failure always originated at a surface or sub-surface flaw and propagates along the plane perpendicular to the loading direction until the final fracture. Figure 8 (a) revealed that failure comes from the defects on the surface of the specimen. Also, Figure 8 (b) shows that the shear lip inclined by 45° near the end of crack propagation and this implies the brittleness of the material.

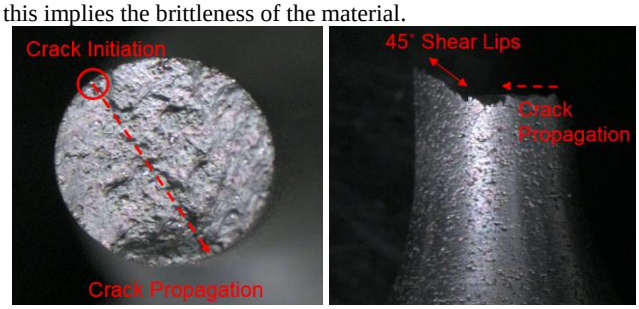


Fig 8: Tensile crack surfaces of as-built of AlSi10Mg (a) Crack propagation (b) Shear lip.

Figure 9 (a) shows the direction of crack propagation for specimens that have been heat-treated (T6). The surface of the specimen shows a lot of small dimples and uniform surface in contrast to the surface of the specimen original material (as-built specimen). Figure 9 (b) shows that the shear lip is not visible as compared to the as-built material. This also implies that the ductility has been introduced into the material itself.

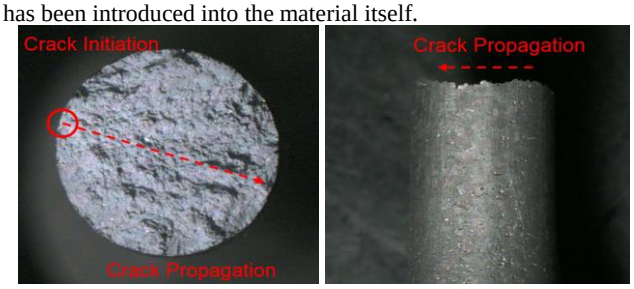


Fig 9: Tensile crack surface of heat-treated (T6) of AlSi10Mg (a) Crack growth (b) Crack propagation

3.4. Fatigue test

Batches of data obtained from the experimental results are plotted based on the stress-life (S-N) method. Figure 10 (a) illustrates the fatigue behaviour of the specimens based on the plot data along with the inclusion of the results from the literature. From the fatigue testing, not a single of the specimens that are tested reaches the endurance limit. This is due to the range of stresses are higher as compared to the heat-treated condition. In the range of high stresses, it can be seen that the improvement in cycle life is quite low.

Figure 10 (b) show a significant increase in the fatigue performance of the specimens that were heat-treated (T6). It can be seen that the increase in the number of cycles is relatively high in all manner of a range of stresses compared to the as-built specimen. Moreover, the performance of the specimen shows very good

fatigue behaviour in a range of low stresses. However, there are no materials tested considered as run-out in the experiment even at the lowest maximum stress which is 143 MPa.

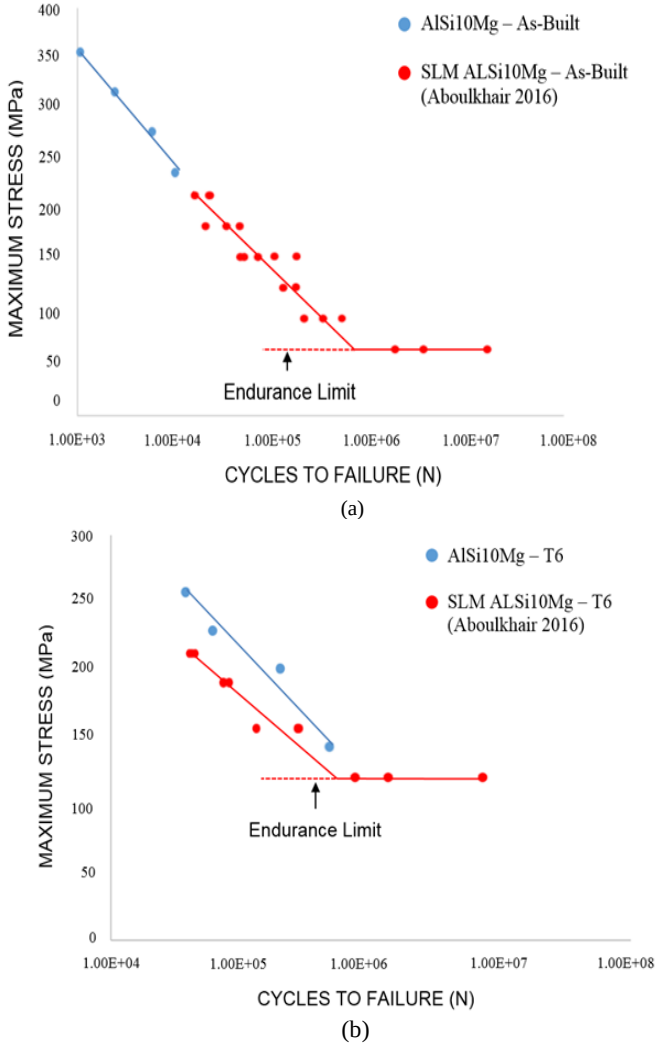


Fig 10: Fatigue behaviour of compared with [9] for (a) as-built (b) heat-treated (T6)

Figure 11 (a) shows the fatigue fracture and crack propagation on the surface of the specimen obtained from the fatigue test. It can be seen that the initial crack is derived from material defects and fracture surface is flat around the area where fatigue crack initiation occurs. According to McMillan and Hertzberg [18], the fracture surface of a fatigue sample is generally flat from a macroscopic appearance viewpoint. A fatigue fracture surface is usually divided into four main regions: namely the fatigue cracked region, the stretched region, the overload fracture region, and the final fracture region. Some of the previous studies combine both fatigue crack and stretched region as the fatigue crack propagation region [16]. Wycisk et al. [19] categorised the types of crack initiation under fatigue loading of SLM parts into two categories: namely failure due to lack of fusion between the layers of powder during sintering or surface defect caused by the poor surface roughness in the as-built specimens.

Figure 11 (b) shows the effect of heat treatment on the fatigue fracture and crack propagation of the specimen under cyclic loading. It can be seen that the fracture surface of the heat-treated specimen is quite flat and uniform. Tiny dimples appear on the fracture surface of the heat-treated specimen as opposed to the observation made on the as-built specimen. It is clear that the heat treatment led to microstructural coarsening.

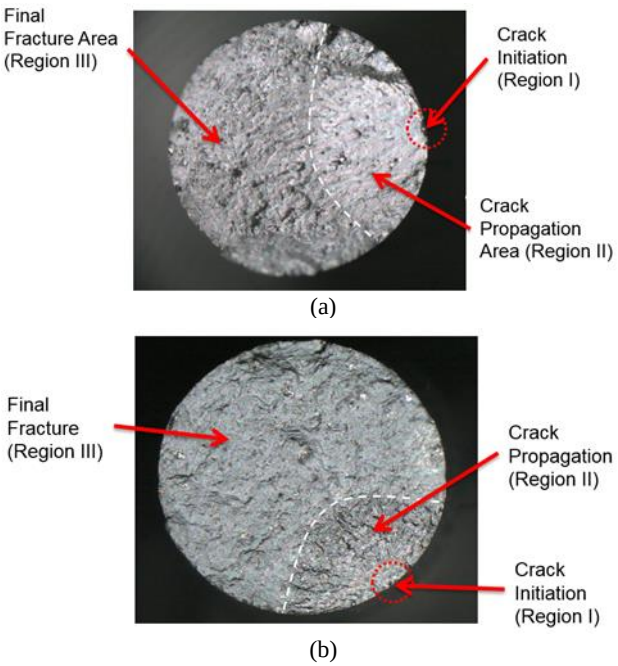


Fig 11: Fatigue fracture surface of (a) as-built (b) heat-treated (T6).

4. Conclusion

Series of experiment and observations have been conducted for the AlSi10Mg material manufactured using DMLS. The microstructural analysis is performed for both as-built and heat-treated (T6). It is observed that the microstructures of the aluminium alloy and silicon particles are segregated uniformly for the as-built condition. However, for the heat-treated (T6) condition, the silicon particles are coarsened and spheroidized into larger particles, thus making it more ductile. The material properties are also compared and characterized through tensile testing for both conditions. The as-built specimen recorded higher UTS compared to T6 specimens respectively at 391.9 MPa and 287.2 MPa. However, the ductility for heat-treated specimen improved by almost double than as-built due to the improvement in the microstructure. The fatigue behaviour also observed. From the results, the fatigue life for heat-treated specimens is improved significantly compared to the as-built condition.

Acknowledgement

The author would like to acknowledge the Universiti Kebangsaan Malaysia (UKM), especially the Laboratory of Computational & Experimental Mechanics (CEM) for allowing the research to be concluded using the High-Performance Computer (HPC). This Research is supported by the Universiti Kebangsaan Malaysia under Dana Impak Perdana. DIP-2016-011.

References

[1] D. C. Hofmann, et al., "Developing Gradient Metal Alloys through Radial Deposition Additive Manufacturing," Scientific Reports (4) 5357 (2014).

[2] V. Matilainen, et al., "Characterization of Process Efficiency Improvement in Laser Additive Manufacturing," Physics Procedia (56) 317-326 (2014).

[3] P. Promoppatum, et al., "Numerical and Experimental Investigations of Micro and Macro Characteristics of Direct Metal Laser Sintered Ti-6Al-4V products," Journal of Materials Processing Technology (2016).

[4] G. Kasperovich and J. Hausmann, "Improvement of fatigue resistance and ductility of TiAl6V4 processed by selective laser melting," Journal of Materials Processing Technology (220) 202-214, 6 (2015).

[5] D. Greitemeier, et al., "Fatigue performance of additive manufactured TiAl6V4 using electron and laser beam melting," International Journal of Fatigue (2016).
[6] A. Riemer, et al., "On the fatigue crack growth behavior in 316L stainless steel manufactured by selective laser melting," Engineering Fracture Mechanics (120) 15-25, 4 (2014).
[7] I. Rosenthal, et al., "Strain rate sensitivity and fracture mechanism of AlSi10Mg parts produced by Selective Laser Melting," Materials Science and Engineering: A (682) 509-517 (2017).
[8] X. Zhao, et al., "Selective laser melting of carbon/AlSi10Mg composites: Microstructure, mechanical and electronical properties," Journal of Alloys and Compounds (665) 271-281(2016).
[9] N. T. Aboulkhair, et al., "The microstructure and mechanical properties of selectively laser melted AlSi10Mg: The effect of a conventional T6-like heat treatment," Materials Science and Engineering: A (667) 139-146 (2016).
[10] E. Brandl, et al., "Additive manufactured AlSi10Mg samples using Selective Laser Melting (SLM): Microstructure, high cycle fatigue, and fracture behavior," Materials & Design (34) 159-169 (2012).
[11] M. S. Shaari, et al., "Prediction of fatigue crack growth for semi-elliptical surface cracks using S-version fem under tension loading," Journal of Mechanical Engineering and Sciences (10) 2375-2386 (2016).
[12] M. R. M. Akramin, et al., "Surface crack analysis under cyclic loads using probabilistic S-version finite element model," Journal of the Brazilian Society of Mechanical Sciences and Engineering (37) 1851-1865 (2015).
[13] L. Thijs, et al., "Fine-structured aluminium products with controllable texture by selective laser melting of pre-alloyed AlSi10Mg powder," Acta Materialia (61) 1809-1819 (2013).
[14] D. Manfredi, et al., "From Powders to Dense Metal Parts: Characterization of a Commercial AlSiMg Alloy Processed through Direct Metal Laser Sintering," Materials (6) 856 (2013).
[15] T. M. Mower and M. J. Long, "Mechanical behavior of additive manufactured, powder-bed laser-fused materials," Materials Science and Engineering: A (651) 198-213 (2016).
[16] C. R. Brooks and A. Choudhury, Failure Analysis of Engineering Materials: McGraw-Hill Education (2002).
[17] N. T. Aboulkhair, I. Maskery , C. Tuck , I. Ashcroft and N.M. Everitt, "Improving the fatigue behaviour of a selectively laser melted aluminium alloy: Influence of heat treatment and surface quality," Materials & Design, (104) (2002).
[18] J. McMillan and R. Hertzberg, "Application of electron fractography to fatigue studies," in Electron Fractography, ed: ASTM International (1968).
[19] E. Wycisk, A. Solbach, S. Siddique, D. Herzog, F. Walther and C. Emmelmann, "Effects of Defects in Laser Additive Manufactured Ti-6Al-4V on Fatigue Properties," Physics Procedia (56) 371-378 (2014).